Comparison of Thermal Stability of Epitaxially Grown (La0.5Sr0.5)CoO3 and (La0.6Sr0.4)MnO3 Thin Films Deposited on Si Substrate

doi: 10.4028/www.scientific.net/KEM.445.160

Comparison of Thermal Stability of Epitaxially Grown $(La_{0.5}Sr_{0.5})CoO_3$ and $(La_{0.6}Sr_{0.4})MnO_3$ Thin Films Deposited on Si Substrate

Shigeki Sawamura[1], Naonori Sakamoto[1], Desheng Fu[1], Kazuo Shinozaki[2], Hisao Suzuki[1], Naoki Wakiya[1,a]

[1]Department of Materials Science and Chemical Engineering, Shizuoka University, 3-5-1 Johoku, Naka-ku, Hamamatsu 432-8561, Japan

[2]Department of Metallurgy and Ceramics Science, Tokyo Institute of Technology, 2-12-1 O-okayama, Meguro-ku, Tokyo 152-8550, Japan

[a] tnwakiy@ipc.shizuoka.ac.jp

Keywords: Bottom electrode; Thin film; Epitaxial growth; PLD; Multiferroic

Abstract. Thermal stability of bottom electrode thin films $(La_{0.5}Sr_{0.5})CoO_3$ (LSCO) and $(La_{0.6}Sr_{0.4})MnO_3$ (LSMO) were investigated. The crystallization and surface morphology of the heterostructure were characterized using x-ray diffraction and atomic force microscopy. Resistivity of the LSCO thin film was 25 Ωcm. However, the resistivity of LSCO thin film increases sharply with annealing temperature. The LSMO thin film has high resistivity (100 mΩcm). The film does not decompose after thermal processing at 900 °C. To confirm thermal stability, we examined the effect of post annealing at various temperatures on the morphology and resistivity. Results showed that LSMO has higher thermal stability than that of LSCO.

>>>>Confirm that this journal uses a space before °C

Introduction

A multiferroic concept has been accepted recently. Multiferroic materials are of two categories: materials that show ferroelectricity and ferromagnetism (ferrimagnetism) simultaneously in one compound, such as $TbMnO_3$ [1], $DyMnO_3$ [2], $TbMn_2O_5$ [3], $BiFeO_3$ [4], and $Ba_{0.5}Sr_{1.5}Zn_2Fe_{12}O_{22}$ [5]; and composites of ferroelectric and ferromagnetic materials. These film morphologies are of two groups, as presented in Fig. 1: (a) 2-2 type and (b) 1-3 type. The 2-2 type comprises stacked thin films including a superlattice, and PZT/(La,Sr)MnO_3[6], $BaTiO_3/Fe_3O_4$ [7], and $La_{0.7}Ca_{0.3}MnO_3/BaTiO_3$ [8] belong to this group. The 1-3 type has a characteristic structure in which ferromagnetic (ferroelectric) nanopillars are embedded in the ferroelectric (ferromagnetic) matrix. Zheng et al. first prepared this type: a $BaTiO_3$-$CoFe_2O_4$ composite film in which $CoFe_2O_4$ nanopillars are embedded in the $BaTiO_3$ matrix [9]. Subsequently, many researchers attempted to prepare 1-3 type thin films between ferroelectric perovskites ($BiFeO_3$, $PbTiO_3$) and ferromagnetic spinels ($NiFe_2O_4$, $CoFe_2O_4$) [10–13]. Most studies deposited a composite thin film on a SrTiO single crystal substrate. We grew a $BaTiO_3$-$CoFe_2O_4$ composite thin film epitaxially on a Si substrate [14].

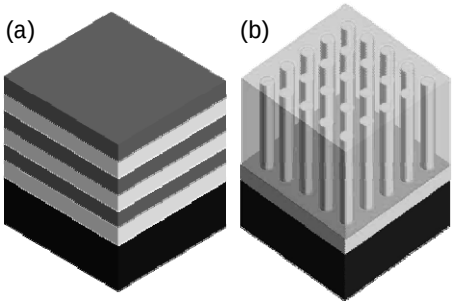

Fig. 1. Schematic of composition in (a) the 2-2 type and (b) 1-3 type

Nevertheless, one problem arose: the bottom electrode. Typical oxide electrodes (such as $(La_{1-x}Sr_x)CoO_3$(LSCO), $LaNiO_3$, and $MgIn_2O_4$) were decomposed or showed semi-conductive electric conduction after thermal processing at temperatures higher than 700 °C. Temperatures

higher than 800 °C are necessary to prepare 1-3 type composite thin films, which require high thermal stability for the bottom electrode. Recently, a widely used bottom electrode showing high thermal stability is $SrRuO_3$(SRO). The SRO perovskite structure enables epitaxial growth on the ferroelectric layer. Many reports have described epitaxially grown SRO thin films, but most epitaxial SRO thin films are deposited on $SrTiO_3$ single crystal. Very few reports describe epitaxial growth on a Si substrate [15]. Another bottom electrode material that is epitaxially grown on a Si(001) substrate is $(La_{1-x}Sr_x)MnO_3$(LSMO). In fact, LSMO shows higher thermal stability than LSCO, but LSMO shows higher resistivity. Therefore, we investigated the bottom electrode, which shows high thermal stability and low lattice mismatch between the buffer layer and bottom electrode layer.

Experimental

In this work, a multilayer-structured thin film was prepared. A Si(100) substrate with natural oxide was cleaned in 2-propanol and used as a substrate. On the Si(100) substrate with native oxide, $Y_{0.15}Zr_{0.85}O_{1.93}$ (YSZ) was used as the initial layer to realize heteroepitaxial growth [16]. A CeO_2 layer was used to adjust the mismatch between YSZ and LSCO and LSMO. The films were deposited using pulsed laser deposition (PLD) with a KrF excimer laser (λ= 248 nm) operated at a 7 Hz repetition rate. A fused silica lens at a 45º angle focused the laser beam on each target. The laser fluence was approximately 2 J/cm^2. The distance between the target and substrate was maintained at 55 mm. Both the target and substrate were rotated during deposition. Table I presents detailed deposition conditions. Ceramic disks of $(La_{0.5}Sr_{0.5})CoO_3$(LSCO) and $(La_{0.6}Sr_{0.4})MnO_3$(LSMO) with stoichiometric composition synthesized using a conventional solid-state reaction were used as targets. The LSCO and LSMO are 100 nm thick. The thin film crystal structure was examined using a precise X-ray diffractometer equipped with a Cu rotating anode (ATX-G; Rigaku Corp. and D8 Advance; Bruker AXS GmbH); the X-ray pole figure and reciprocal space maps were measured. The film morphology was observed using atomic force microscopy (AFM). Electric resistivity of the LSCO and LSMO thin films was measured using a four-probe method and a source measurement unit (236; Keithley Instruments Inc.).

Table I. Deposition conditions of LSCO and LSMO thin films

	Deposition temperature (˚C)	Deposition pressure (Pa)
LSCO	550	0.07
LSMO	700	50

>>>>Figs. 2,3 Use a space before [Use deg and arb. unit as the units

Results and discussion

Figure 2 portrays the 2θ/ω XRD pattern of the LSCO and LSMO thin films on the CeO_2/YSZ buffered Si substrate. This figure shows that all films have a c-axis orientation. To clarify the in-plane orientation relation, pole figure measurements were conducted. Results showed that LSCO and LSMO oxide electrodes are grown epitaxially with 45 deg rotation against Si. Figures 3(a) and 3(b) show the 2θ/ω XRD patterns around the (002) reflection peak

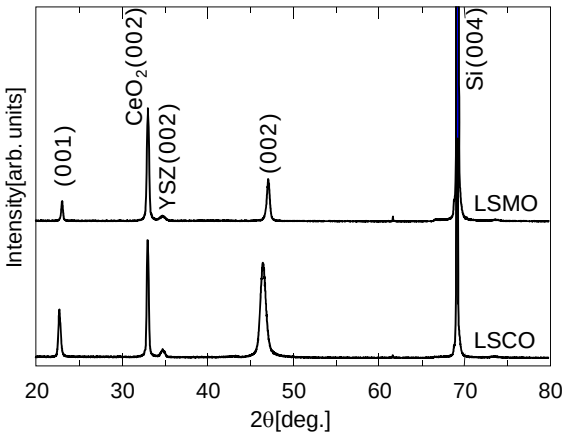

Fig. 2. X-ray diffraction pattern of LSCO and LSMO thin film on CeO_2/YSZ buffered Si(100) substrate.

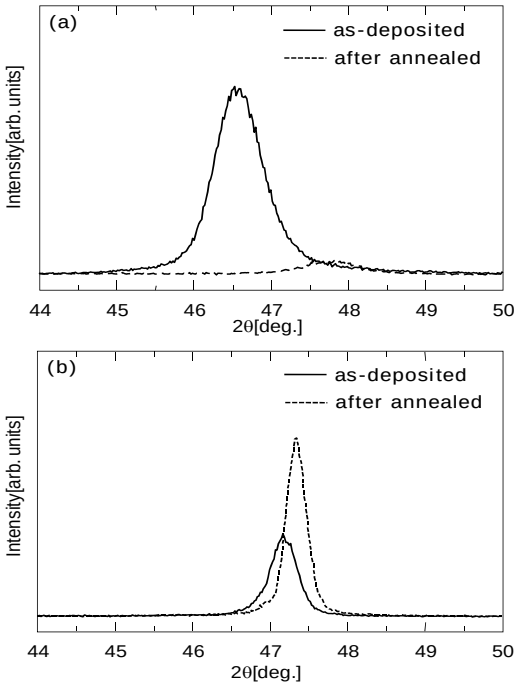

Fig. 3. XRD pattern around the (002) reflections of (a) LSCO and (b) LSMO.

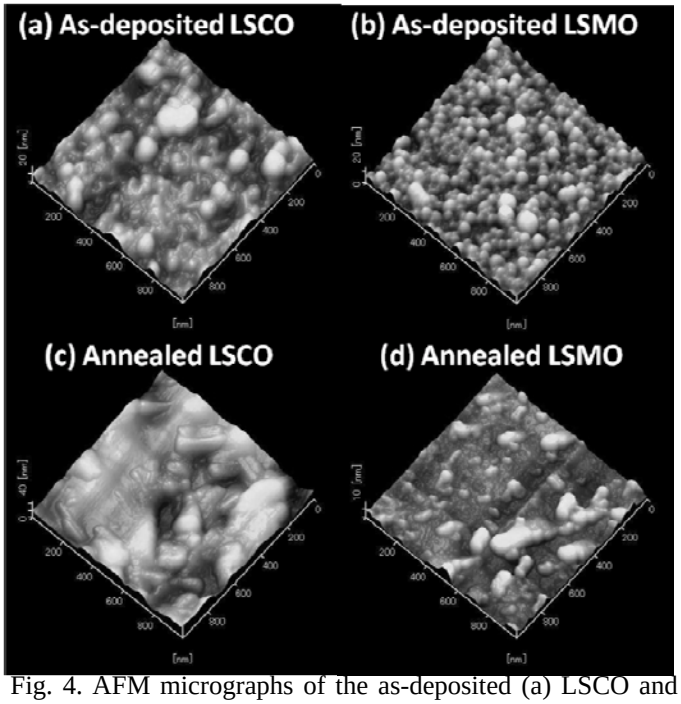

Fig. 4. AFM micrographs of the as-deposited (a) LSCO and (b) LSMO and annealed at 900 °C (c) LSCO and (d) LSMO

before and after annealing in air at 900 °C in air for (a) LSCO and (b) LSMO, respectively. This figure shows that the LSCO decomposed after the annealing. In contrast, the lattice constant of LSMO is lower after the annealing. The lattice constant of as-deposited and after annealing LSMO are, respectively, 0.3850 nm and 0.3837 nm. This change suggests that as-deposited LSMO contains oxygen vacancies, and that the vacancy would be filled by oxygen to decrease the lattice constant.

Figure 4 presents AFM (tapping mode) images of the surface morphology of LSCO and LSMO thin films before and after annealing at 900 °C in air. The root-mean-square roughness (RMS) values of Figs. 4(a)–4(d) are, respectively, 4.9, 3.7, 6.2, and 2.4 nm. Annealing decreased the surface roughness of LSMO thin film, but post-annealing increased the LSCO thin film roughness.

Figure 5 depicts the change of resistivity with annealing temperature of LSCO and LSMO thin films. This figure shows that thermal stability of oxide electrodes has different characteristics. For LSCO, the resistivity of as-deposited film is 24 mΩcm. However, the resistivity increases with annealing temperature up to 115 Ωcm. Figure 3 shows that this increase of resistivity would be derived by the decreased carrier concentration and increased surface roughness. Actually, LSMO shows a tendency by which the resistivity decreased with annealing temperature. This is derived by the increased mobility from decreasing surface roughness. Resistivity of the LSMO thin film after annealing at 900 °C is 18 mΩcm, which is smaller than resistivity of as-deposited LSCO thin film. Results reflect that LSMO has higher thermal stability than that of LSCO, and that LSCO tends to deteriorate by annealing, which suggests that improvements of preparation conditions are necessary to use LSCO at high temperatures. Resistivity of LSMO thin films is higher than that of SRO thin

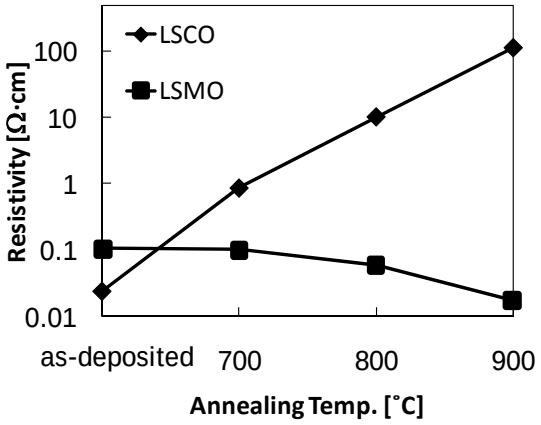

Fig. 5. Resistivity vs. annealing temperature of LSCO and LSMO thin films.

film; however, thermal stability of LSMO is comparable with that of SRO.

Conclusions

We deposited LSCO and LSMO thin films on CeO_2/YSZ buffered Si(100) substrate using pulsed laser deposition. The AFM measurements of LSCO and LSMO thin films revealed that post annealing increases the LSCO roughness. In contrast, the LSMO thin film roughness is decreased after post annealing. The LSCO thin film resistivity increased dramatically with annealing temperature. In contrast, the LSMO thin film resistivity shows a decrease concomitantly with increasing annealing temperature. Resistivity of the LSMO thin film after annealing at 900 °C is 18 mΩcm, which is less than the resistivity of as-deposited LSCO thin film. The LSMO thin film shows higher thermal stability and lower resistivity than the LSCO thin film. Results show that the LSMO thin film resistivity is higher than that of the SRO thin film. However, the thermal stability of LSMO is comparable with that of SRO.

References

[1] T. Kimura, T. Goto, H. Shintani, K. Ishizaka, T. Arima, and Y. Tokura: Nature 426 (2003) 55.

[2] T. Kimura, G. Lawes, T. Goto, Y. Tokura, and A. P. Ramirez: Phys. Rev. B 71 (2005)224425.

[3] N. Hur, S. Park, P. A. Sharma, J. S. Ahn, S. Guha, and S. W. Cheong: Nature 429 (2004) 392

[4] J. Wang, J. B. Neaton, H. Zheng, V. Nagarajan, S. B. Ogale, B. Liu, D. Viehland, V. Vaithyanathan, D. G. Schlom, U. V. Waghmare, N. A. Spaldin, K. M. Rabe, M. Wuttig, and R. Ramesh: Science 299 (2002) 1719.

[5] N. Momozawa and Y. Yamaguchi: J. Phys. Soc. Jpn. 62 (1993) 1292

[6] H. Tabata and T. Kawai: IEICE Trans. Electron. E-80C (1997) 918

[7] M. Ziese, A. Bollero, I. Panagiotopoulos, and N. Moutis: Appl. Phys. Lett. 88 (2006) 212502.

[8] M. P. Singh, W. Prellier, L. Mechin, C. Simon, and B. Raveau: J. Appl. Phys. 99 (2006) 024105.

[9] H. Zheng, J. Wang, S. E. Lofland, Z. Ma, L. M. Ardabili, T. Zhao, L. S. Riba, S. R. Shinde, S. B. Ogale, F. Bai, D. Viehland, Y. Jia, D. G. Schlom, M. Wuttig, A. Roytburd, and R. Ramesh: Science 303 (2004) 661.

[10] W. Chen, Z. H. Wang, C. Ke, W. Zhu, and O. K. Tan: Mater. Sci. Eng. B162 (2009) 47.

[11] I. Levin, J. Li, J. Slutsker, and A. L. Roytburd: Adv. Mater. 18 (2006) 2044.

[12] Q. Zhang, R. Yu, S. P. Crane, H. Zheng, C. Kisielowski, and R. Ramesh: Appl. Phys. Lett. 89 (2006) 172902.

[13] R. Muralidharan, N. Dix, V. Skumryev, M. Varela, F. Sánchez, and J. Fontcuberta: J. Appl. Phys. 103 (2008) 07E301.

[14] S. Sawamura, N. Wakiya, N. Sakamoto, K. Shinozaki, and H. Suzuki: Jpn. J. Appl. Phys. 47 (2008) 7603.

[15] H-Y. Go “Studies on crystal orientation and electrical properties of epitaxial ferroelectric thin films on Si and YSZ substrates by introducing buffer layers,” (Ph. D. thesis, Tokyo Institute of Technology, 2009)

[16] D. B. Fenner, D. K. Fork, G. A. N. Connell, J. B. Boyce, F. A. Ponce, J. C. Tramontana, A. M. Viano, and T. H. Geballe: Mater. Res. Soc. Symp. Proc. 191 (1990) 187.